Available online at www.sciencedirect.com
SCIENCE DIRECT®
Journal of Solid State Chemistry 171 (2003) 401–407
JOURNAL OF SOLID STATE CHEMISTRY
http://elsevier.com/locate/jssc

Luminescence investigation of Eu^{3+} ion in the $RE_2(WO_4)_3$ matrix (RE = La and Gd) produced using the Pechini method

Cláudia A. Kodaira, Hermi F. Brito,* and Maria Cláudia F.C. Felinto

Departamento de Química Fundamental, Instituto de Química, Universidade de São de Paulo, C.P. 26077, São Paulo-SP, Brazil

Received 3 May 2002; received in revised form 15 July 2002; accepted 23 July 2002

Abstract

The preparation, characterization and photoluminescent study of Eu^{3+} ions doped into the $RE_2(WO_4)_3$ matrix (RE = La and Gd), which was produced by the Pechini method at 750°C are reported. This method is based on polyesterification between citric acid and ethylene glycol, producing a material at low temperature. The X-ray diffraction patterns of the powder materials show the characteristic lines of the rare-earth tungstates. The infrared data are compatible with a T_d point group symmetry for the tungsten atom units in both compounds. The excitation spectra of these systems ($\lambda_{em} = 615$ nm) showed an intense broad band with maximum at 265 nm related to the O→W ligand-to-metal charge-transfer state. The emission spectra of the Eu^{3+} ion ($\lambda_{excitation} = 393$ nm) presented peaks arising from the $^5D_J \rightarrow {}^7F_{J'}$ transitions ($J = 0$–3 and $J' = 0$–4) and are compatible with a C_{nv} symmetry. The values of Ω_2 experimental intensity parameters (25.8×10^{-20} and 21.5×10^{-20} cm^2 for La^{3+} and Gd^{3+} ions, respectively), reflect the hypersensitive character of the $^5D_0 \rightarrow {}^7F_2$ transition and indicate that the Eu^{3+} ion is in a highly polarizable chemical environment, suggesting a considerable covalent character of the metal–donor atom interaction. The high emission quantum efficiencies of the $RE_2(WO_4)_3$:Eu^{3+} materials (68% for La^{3+} and 64% for Gd^{3+}) suggest that these systems are promising phosphors. The CIE chromaticity coordinates indicate that they are comparable to those of the commercially available red phosphor in cathode ray tubes.

Keywords: Lanthanum; Gadolinium and europium ions; Tungstate; Pechini method; LMCT states; Photoluminescence

1. Introduction

Nowadays, phosphors find a wide variety of applications such as in radiation detectors and visual displays. The introduction of trivalent rare-earth ions (RE^{3+}) in matrices as luminescent centers has been an improvement in the field of luminescent materials [1].

The optical properties of the Eu^{3+} ion doped into matrices are important for the preparation of luminescent inorganic materials due to several advantages: (a) The pure red emission of the Eu^{3+} ion, (b) the Eu^{3+} ion is used as a general photoluminescent probe, (c) the emitting level $^5D_0$ and the ground state $^7F_0$ are non-degenerate, (d) the magnetic dipole $^5D_0 \rightarrow {}^7F_1$ transition is allowed, (e) the hypersensitive transition $^5D_0 \rightarrow {}^7F_2$ can give information about the covalent character of the rare-earth ligand bond. The luminescence decay time of the emitting $^5D_0$ level (ms) is longer.

Nassau et al. [2] gave a survey of the structures of tungstates and molybdates with the formula $RE_2(WO_4)_3$ along the rare-earth series. Borchardt [3] prepared the rare-earth tungstates with similar purposes and Templeton and Zalkin [4] studied the crystal structure of europium tungstate. Since then, systems containing tungstate and the europium ion have been reported extensively in the literature [5–8]. A solid-state reaction is most often used to prepare europium tungstate. We have used the Pechini method to prepare the $Eu_2(WO_4)_3$ compound [9]. This technique [10–12] has been utilized due to low cost and versatility, allowing preparation of oxide samples at low temperatures, where an α-hydroxycarboxylic acid is used to chelate various cationic precursors by forming a polybasic acid. In the presence of a polyhydroxyl alcohol these chelates react with the alcohol to form organic esters and water by-products. When the mixture is heated polyesterification occurs.

*Corresponding author. Fax: +55-11-3815-5579.
E-mail address: hefbrito@iq.usp.br (H.F. Brito).

0022-4596/03/$ - see front matter © 2003 Elsevier Science (USA). All rights reserved.
doi:10.1016/S0022-4596(02)00221-9

Afterwards, the excess solvent is removed and a solid resin is formed and, with increasing temperature the desired solid product is obtained.

The aim of this work is to prepare the $RE_2(WO_4)_3$ matrices doped with Eu^{3+} ion (RE = La and Gd) using the Pechini method and to investigate their photoluminescent properties. An emission quenching phenomenon observed for the $^5D_{1,2,3}$ manifolds, under excitation at the ligand-to-metal charge-transfer (LMCT) states, is discussed and interpreted as a resonance crossover between the LMCT states and the $^5D_{1,2,3}$ levels. The relatively high emission quantum efficiency of 68% and 64% for the emitting $^5D_0$ level of the materials containing La and Gd, respectively, when compared to the $Eu_2(WO_4)_3$ compound ($\eta = 19\%$), is interpreted as a lower quenching also due to the LMCT states.

2. Experimental section

2.1. Preparation of the $RE_2(WO_4)_3$:Eu^{3+} systems

The $RE_2(WO_4)_3$:Eu^{3+} were prepared by the Pechini method [10–12]. The starting materials were ammonium tungstate (99.999%, Acros), RE_2O_3 (RE = La, Eu, Gd) (99.9%, Aldrich), ethylene glycol (99.5%, Merck) and citric acid (99.5%, Merck). The Eu^{3+} ion was doped in the matrix with a concentration of 5 mol%. Firstly, the $(NH_4)_2WO_4$ was dissolved in a heated aqueous solution ($\sim$60°C), adjusting the pH to be 7.0 with ammonium hydroxide. Secondly, rare-earth oxides were dissolved with nitric acid aqueous solution. The ethylenediaminetetraacetic acid (EDTA) was then added to the solution containing the RE^{3+} ions to form a stable RE complex. Ammonium tungstate is added to the mixture and the pH is adjusted to 5 with ammonium acetate, so that the WO_4^{2-} ions remain in the solution [13].

To this clear solution, the citric acid and ethylene glycol were added under continuous stirring and heating in water bath, adjusting the pH to $\sim$5 with $CH_3CO_2NH_4$. The resulting brown transparent resin was heated at 200°C for 2 h, resulting in a fluffy black mass, which was ground into a powder (precursor). In a final step, the precursor was calcined at 750°C for 4 h producing the $RE_2(WO_4)_3$:Eu as a white powder.

2.2. Measurements

The powder X-ray diffraction patterns from 2° to 70° (2θ) were recorded on a Philips diffractometer model X'PERT-MPD using Cu$K\alpha$ radiation (40 kV and 40 mA).

Thermogravimetric (TG) curves were obtained with a TG-50 thermobalance (Shimadzu), using platinum crucibles with 2.7 mg of the sample, under a continuous air flow (50 mL min^{-1}), at a heating rate of 10°C min^{-1}.

Infrared data were recorded on a Bomem MB 100 spectrometer by averaging 96 scans with a resolution of 4 cm^{-1}. Samples were physically mixed with KBr and pressed into self-supporting wafers. These measurements were made at room temperature in the 1200–350 cm^{-1} range.

The excitation and emission spectra at room and liquid nitrogen temperature were collected at an angle of 22.5° (front face) in a spectrofluorimeter (SPEX-Fluorolog 2) with double grating 0.22 m monochromator (SPEX 1680), and a 450 W Xenon lamp as the excitation source. This apparatus was controlled by a DM3000F spectroscopic program and computer. The solid samples were maintained in a quartz dewar flask at 77 K. The lifetime measurements were recorded at 298 K using the phosphorimeter (SPEX 1934D) accessory coupled with the spectrofluorimeter.

3. Results and discussion

3.1. Characterization

X-ray diffraction patterns of the powders calcined at 750°C are typical of monoclinic lanthanum and gadolinium tungstate (JCPDS card #15-0438 and #23-1076, respectively). According to Ref. [4] the two compounds are isostructural and belong to space group $C_{2h}^6 - C2/c$ with distorted scheelite structures.

The TG curve of the $La_2(WO_4)_3$:Eu powder precursor (Fig. 1) showed a thermal behavior similar to that of $Gd_2(WO_4)_3$:Eu (figure not shown). The weight loss of 4%, in the temperature interval from 25°C to 200°C, was associated with water loss, while the weight loss of 80%, in the range from 200°C to 750°C, is related to the decomposition of the organic constituents. In the temperature interval from 750°C to 900°C no weight loss was observed (Fig. 1), therefore, the calcinations of

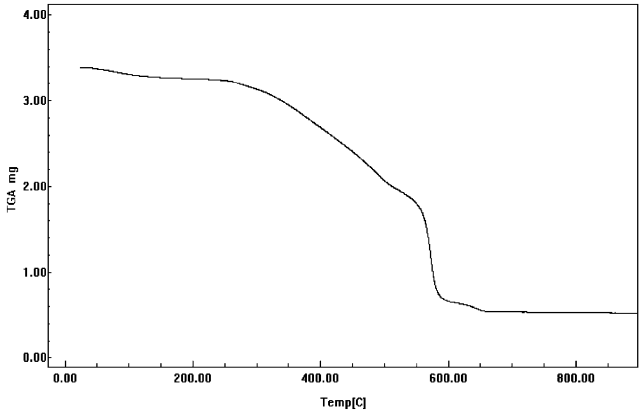

Fig. 1. TG curve of the $La_2(WO_4)_3$:Eu precursor powder in air flow of 50 mL min^{-1}.

the ground precursor powders at 750°C suggest the formation of the $RE_2(WO_4)_3$:Eu^{3+}.

The vibrational spectrum of the $La_2(WO_4)_3$ has been assigned previously by Burcham and Wachs [14] by assuming a tetrahedral, T_d, point group symmetry as an approximation to the actual, non-ideal symmetry of WO_4 units. The crystal structure data for $Eu_2(WO_4)_3$ and $La_2(WO_4)_3$ indicate the isomorphism of these compounds and also show the tungsten atoms residing on two different types of sites in which each W atom is surrounded by four oxygen atoms [4]. One WO_4 unit is close to being a geometrically regular tetrahedron and the other unit is much more distorted. In our systems the following frequencies were observed in $La_2(WO_4)_3$:Eu^{3+} (944m, 936sh, 870sh, 846s, 810s, 760sh, 735s, 678s, 471w, 448w, 404w, 375w) cm^{-1} and in $Gd_2(WO_4)_3$:Eu^{3+} (949s, 939sh, 861s, 806s, 755sh, 738s, 693s, 485w, 463w, 421w, 391w, 364w) cm^{-1} (where s = strong, m = medium, w = weak sh = shoulder). The similarity between the IR data of the $RE_2(WO_4)_3$ matrices doped with Eu^{3+} ion and those of the $La_2(WO_4)_3$ [14] suggests the presence of two different WO_4 units.

3.2. Photoluminescent study

Fig. 2 shows the excitation spectra of $RE_2(WO_4)_3$:Eu^{3+} (RE^{3+} = La and Gd) under emission at 615 nm, at liquid nitrogen temperature. In the 310–590 nm spectral range, both spectra display sharp lines from

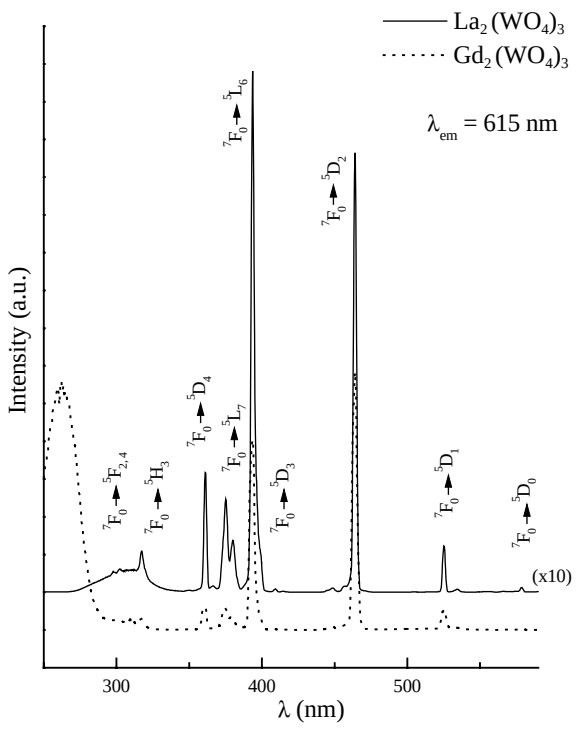

Fig. 2. Excitation spectra of the $La_2(WO_4)_3$:Eu^{3+} (solid line) and $Gd_2(WO_4)_3$:Eu^{3+} compounds (dot line) with the emission monitored at 615 nm at liquid nitrogen temperature.

the $^7F_0 \rightarrow {}^5L_J$ ($L = D, F, H$ and L, where $J = 0-7$) transitions of the Eu^{3+} ion (Table 1). Both spectra exhibit similar profiles except for two specific features: (a) the spectrum of $La_2(WO_4)_3$:Eu^{3+} compound presents a low-intensity broad band, in the interval of 250–330 nm attributed to O→W LMCT and O→Eu^{3+} LMCT [6] with overlap with the narrow $^7F_0 \rightarrow {}^5F_{2,4}$ and $^5H_3$ transitions from the Eu^{3+} ion and (b) the $Gd_2(WO_4)_3$:Eu^{3+} compound shows a high-intensity broad band at 265 nm while the band at around 310 nm shows low-intensity attributed to O→W and O→Eu^{3+} LMCT, respectively. Besides these features, this excitation spectrum can also contain $^8S \rightarrow {}^6I$ excitation weak lines of Gd^{3+} ion (~275 nm) [15], which exciting radiation is masked by the tungstate group. This group partly transfers its energy to Eu^{3+} and Gd^{3+} ions, which in turn can transfer to Eu^{3+} ion. The narrow bands arising from the $^8S \rightarrow {}^6P$ transition are overlapping at about 310 nm.

Fig 3a presents two broad bands around 265 (high intensity) and 310 nm (low intensity) assignment to the O→W LMCT from WO_4 units in the $Gd_2(WO_4)_3$ compound (without Eu^{3+} ion). The inset (Fig. 3a) shows the amplified spectrum in the range from 305 to 320 nm of the O→W LMCT band. These spectral data confirm the presence of the high-intensity band around 265 nm for $Gd_2(WO_4)_3$ doped with Eu^{3+} compound in Fig. 2. Excitation into the tungstate group (265 nm) results in a broad emission band, centered at 505 nm.

The emission spectra of the $RE_2(WO_4)_3$:Eu^{3+} compounds recorded in the 420–720 nm spectral range under excitation monitored in the O→Eu^{3+} LMCT (310 nm), at 77 K, are given in Fig. 4. It displays the sharp lines of the Eu^{3+} ion from 570 to 720 nm for both compounds. However, only the La compound presents a low-intensity broad band from 420 to 570 nm assigned to O→W ligand-to-metal charge-transfer states. As can be seen, the relative intensities spectral profiles of the $^5D_0 \rightarrow {}^7F_J$ transitions ($J = 0-4$) are different, indicating that the Eu ions, are in similar chemical environments in the two compounds. This behavior can be explained by the differences between the ionic radii of La^{3+} (1.023 Å) and Gd^{3+} (0.938 Å) ion. It is possible that the La^{3+} ion can be distorting the tungstate structures due to its larger ionic radius, while the Gd^{3+} ion, being smaller, can be forming almost regular tetrahedral tungstate units.

It is interesting to notice that in Fig. 4 there are no bands arising from the ^5D_J levels ($J = 1, 2$ and 3) emitting levels because the low-lying charge-transfer states skips the higher-lying ^5D_J levels [16] during the relaxation process as in Fig. 6 reported in Ref. [6]. On the other hand, when the emission spectra (Table 1) of the $RE_2(WO_4)_3$:Eu^{3+} (RE^{3+} = La and Gd) are recorded under excitation at 393.5 nm ($^7F_0 \rightarrow {}^5L_6$ of Eu^{3+} ion), emission bands corresponding to the

Table 1
Transition energies of the $^5D_J \rightarrow {}^7F_{J'}$ manifolds (in cm^{-1}) observed in the excitation and emission spectra of the $La_2(WO_4)_3$:Eu^{3+} compound at liquid nitrogen temperature

Excitation data		Emission data					
Transition	Energy (cm^{-1})	Transition	Energy (cm^{-1})	Transition	Energy (cm^{-1})	Transition	Energy (cm^{-1})
$^7F_0 \rightarrow {}^5F_4$	33 591	$^5D_3 \rightarrow {}^7F_3$	22 512		19 639	$^5D_0 \rightarrow {}^7F_1$	16 943
$^7F_0 \rightarrow {}^5F_2$	33 091		22 432	$^5D_2 \rightarrow {}^7F_3$	19 608		16 909
$^7F_0 \rightarrow {}^5H_3$	31 496				19 554		16 818
$^7F_0 \rightarrow {}^5D_4$	27 701		21 683				
	27 270	$^5D_2 \rightarrow {}^7F_0$	21 580	$^5D_1 \rightarrow {}^7F_0$	19 026		16 340
$^7F_0 \rightarrow {}^5L_7$	26 660		21 533			$^5D_0 \rightarrow {}^7F_2$	16 271
	26 323	$^5D_3 \rightarrow {}^7F_4$	21 468		18 699		16 218
$^7F_0 \rightarrow {}^5L_6$	25 419		21 422	$^5D_1 \rightarrow {}^7F_1$	18 678		16 113
$^7F_0 \rightarrow {}^5D_3$	24 432		21 368		18 580		
	24 114		21 322			$^5D_0 \rightarrow {}^7F_3$	15 399
$^7F_0 \rightarrow {}^5D_2$	22 487				18 103		15 323
	22 292	$^5D_2 \rightarrow {}^7F_1$	21 160		18 057		
	21 896		21 035	$^5D_1 \rightarrow {}^7F_2$	18 031		14 459
	21 542				17 979	$^5D_0 \rightarrow {}^7F_4$	14 413
$^7F_0 \rightarrow {}^5D_1$	19 044		20 585		17 902		14 351
	18 723	$^5D_2 \rightarrow {}^7F_2$	20 542				14 302
$^7F_0 \rightarrow {}^5D_0$	17 277		20 483	$^5D_0 \rightarrow {}^7F_0$	17 265		14 273
			20 433				14 253
			20 400	$^5D_1 \rightarrow {}^7F_3$	17 153		14 205
			20 358		17 077		

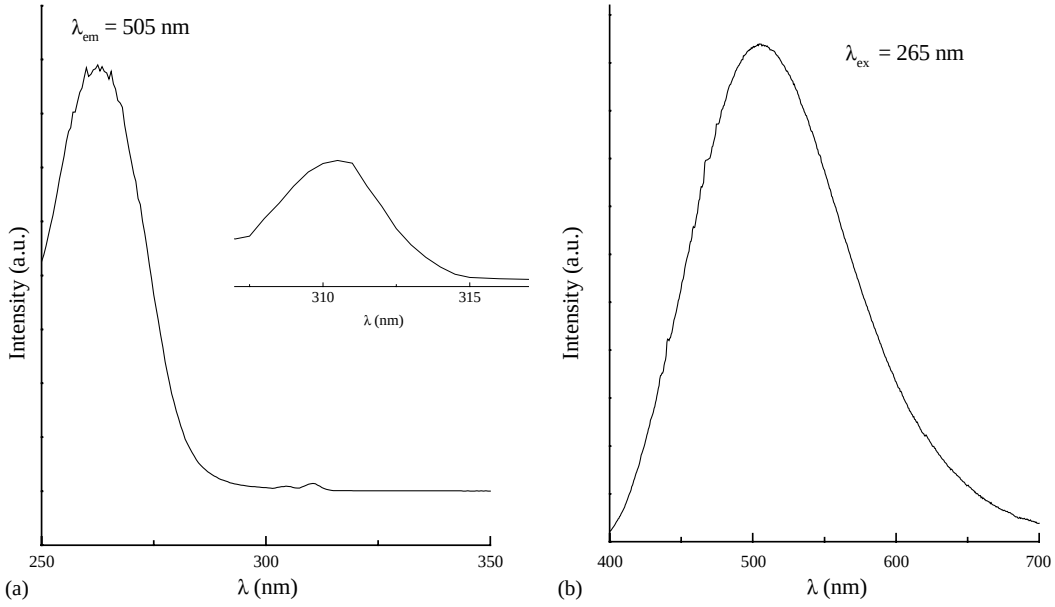

Fig. 3. Luminescence spectra of WO_4^{2-} in the $Gd_2(WO_4)_3$ compound at 77 K: (a) excitation spectra recorded in the range from 250 to 350 nm under emission at 500 nm and (b) emission spectrum obtained in the range from 400 to 700 nm when excited at 260 nm.

$^5D_J \rightarrow {}^7F_J$ electronic transitions (where $J = 1-3$ and $J' = 0-4$) are observed in the range of 420–570 nm (Fig. 5a).

The $^5D_0 \rightarrow {}^7F_0$ transition shows only one peak for the two systems, suggesting the existence of one site symmetry for the Eu^{3+} ion chemical environment (Fig. 5b). These results are also in agreement with the single-exponential behavior in the luminescence decay curves of the emitting $^5D_0$ level. The lifetime recorded at room temperature for the $^5D_0$ excited state of the Eu^{3+} ion in $RE_2(WO_4)_3$:Eu^{3+} are longer than for $Eu_2(WO_4)_3$ (Table 2).

The emission spectra of the Eu^{3+} doped systems show that the $^5D_0 \rightarrow {}^7F_1$ transition (Fig 5b) splits into three

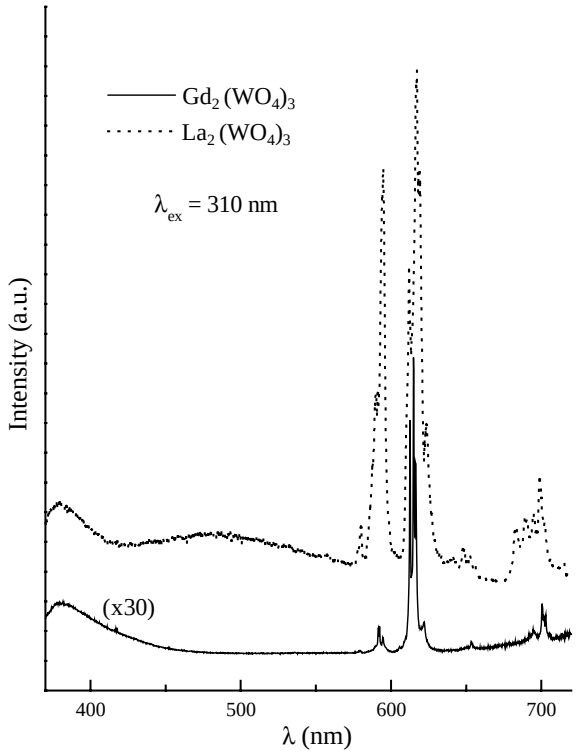

Fig. 4. Emission spectra of $La_2(WO_4)_3$:Eu^{3+} (dot line) and $Gd_2(WO_4)_3$:Eu^{3+} (solid line) compounds, at 77 K ($\lambda_{ex} = 310$ nm).

peaks confirming with the existence of a single local low symmetry chemical environment for Eu^{3+} ion. Fig. 5b also presents the most intense emission band attributed to the hypersensitive $^5D_0 \rightarrow {}^7F_2$ transition, that splits in four bands (Table 1). The peaks arising from the $^5D_J \rightarrow {}^7F_{J'}$ transitions ($J = 0-3$ and $J' = 0-4$) of the Eu^{3+} ion are compatible with a C_{nv} site symmetry.

The luminescence behavior of the Eu^{3+} ion into the $RE_2(WO_4)_3$ can be investigated by the radiative and non-radiative contributions to the decay rates from the emitting level, $^5D_0$ using the $^5D_0 \rightarrow {}^7F_2$ and $^5D_0 \rightarrow {}^7F_4$ transitions to determine the $\Omega_\lambda (\lambda = 2$ and $4)$ experimental intensity parameters by taking the $^5D_0 \rightarrow {}^7F_1$ transition as the reference. The Ω_6 intensity parameter was not included in this study since the $^5D_0 \rightarrow {}^7F_6$ transition could not be observed. The Einstein coefficient of spontaneous emission [17–21], A, in this case is given by Carnall et al. [22]

$$A_{0-\lambda} = \frac{4e^2\omega^3}{3\hbar\, c^3} \quad \chi \sum_{\lambda=2,4} \Omega_\lambda \left\langle {}^5D_0 \middle| U^{(\lambda)} \middle| {}^7F_J \right\rangle^2, \tag{1}$$

where $\chi = n_0(n_0^2+2)^2/9$ is the Lorentz local field correction. The square reduced matrix elements are obtained from Ref. [22], and an average index of refraction equal to 1.5 is used [18]. The $A_{0-\lambda}$ values

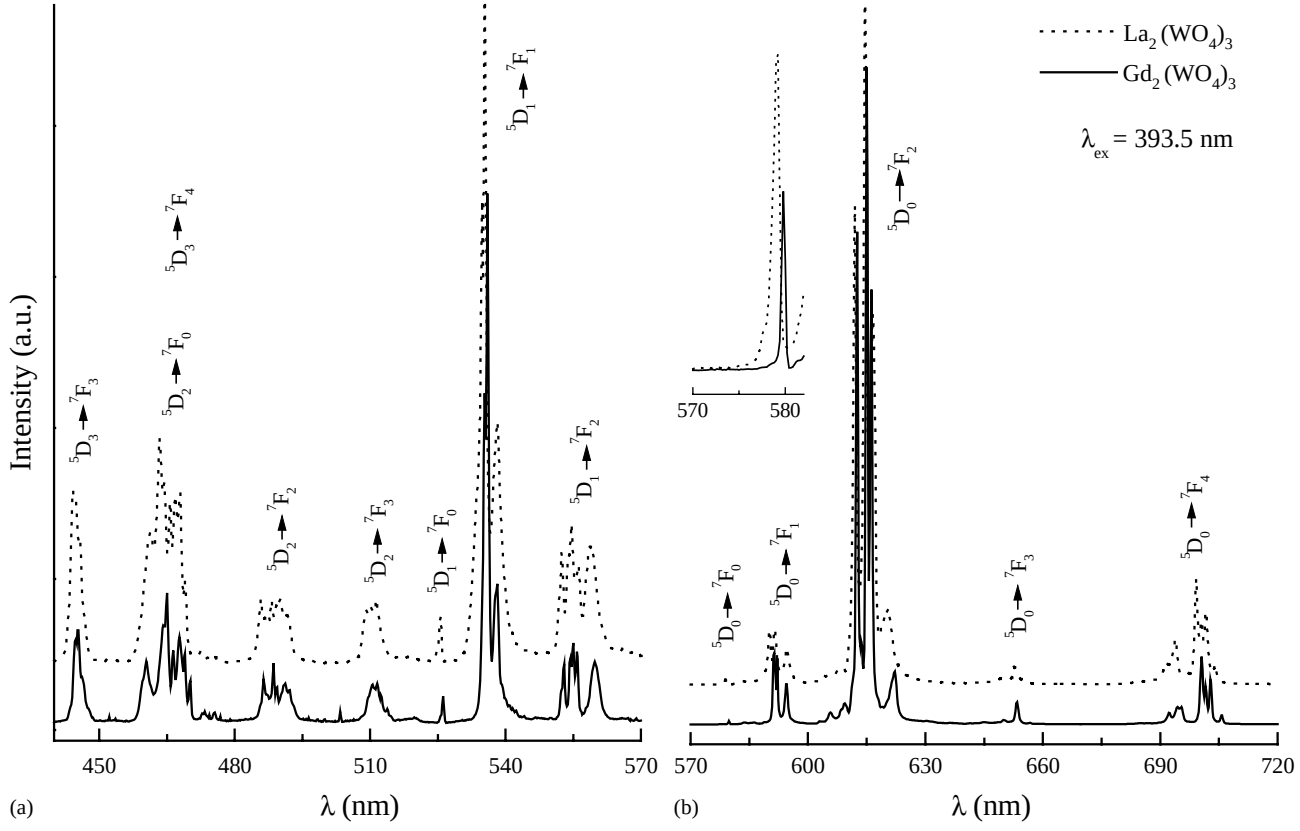

Fig. 5. Emission spectra of the $La_2(WO_4)_3$:Eu^{3+} and $Gd_2(WO_4)_3$:Eu^{3+} compounds with the excitation monitored at 393 nm at 77 K: (a) range from 250 to 570 nm and (b) range from 570 to 720 nm.

Table 2
Experimental intensity parameters (Ω_λ), emission quantum efficiency (η), lifetime (τ), non-radiative (A_{nrad}), radiative (A_{rad}) and total (A_{total}) rates for the $La_2(WO_4)_3$:Eu^{3+} and $Gd_2(WO_4)_3$:Eu^{3+} compounds, at room temperature

Compounds	A_{rad} (s^{-1})	A_{nrad} (s^{-1})	A_{total} (s^{-1})	Ω_2 (10^{-20} cm^2)	Ω_4 (10^{-20} cm^2)	R_{0-2}	τ (ms)	η (%)	Ref.
$La_2(WO_4)_3$:Eu^{3+}	1024	481	1505	25.8	13.1	0.0015	0.66	68	[a]
$Gd_2(WO_4)_3$:Eu^{3+}	838	471	1309	21.5	9.6	0.0009	0.76	64	[a]
$Eu_2(WO_4)_3$	1048	4477	5525	26.9	12.8	0.0013	0.18	19	[9]
$[Eu(TTA)_3(H_2O)_2]$	1110	2730	3846	33.0	4.6	0.0130	0.26	29	[18]

The R_{0-2} parameter is the ratio between the intensities of the $^5D_0 \rightarrow {}^7F_0$ and $^5D_0 \rightarrow {}^7F_2$ transitions.
[a] This work.

are obtained by using the relation: $A_{0-\lambda} = A_{0-1}(S_{0-\lambda}/S_{0-1})\,(\sigma_\lambda/\sigma_1)$ where $S_{0-\lambda}$ is the area under the curve related to the $^5D_0 \rightarrow {}^7F_\lambda$ transition obtained from the spectral data, σ_λ is the energy barycenter of the $0-\lambda$ transition.

The lifetime (τ), non-radiative (A_{nrad}) and radiative (A_{rad}) rates are related through the following equation: $A_{tot} = 1/\tau = A_{rad} + A_{nrad}$, where the A_{rad} rate obtained by summing over the radiative rates A_{0J} for each $^5D_0 \rightarrow {}^7F_J$ transition is given by $A_{rad} = \sum_J A_{0J}$.

The emission quantum efficiency of the emitting $^5D_0$ level is given by

$$\eta = \frac{A_{rad}}{A_{rad} + A_{nrad}}. \quad (2)$$

In Table 2 the values of the Ω_λ parameters ($\lambda = 2$ and 4) are shown for the $RE_2(WO_4)_3$:Eu^{3+} (RE = La and Gd), $Eu_2(WO_4)_3$ [9] and $[Eu(TTA)_3(H_2O)_2]$ [18] compounds, where TTA = thenoyltrifluoroacetonate. It is noteworthy that the highest value of Ω_2 for the $[Eu(TTA)_3(H_2O)_2]$ complex indicates the highest hypersensitive behavior of the $^5D_0 \rightarrow {}^7F_2$ transition. Consequently, the Eu^{3+} ions in the tungstate systems are in a less polarizable environment than in Eu(TTA)-complex, suggesting a smaller electric dipole character to the $^5D_0 \rightarrow {}^7F_2$ transition for the $Gd_2(WO_4)_3$:Eu^{3+} compound. A comparison between the Ω_2 parameters for the tungstate systems (Table 2) shows that the Eu^{3+} ion in the $La_2(WO_4)_3$:Eu^{3+} and $Eu_2(WO_4)_3$ systems presents higher Ω_2 values than in Gd^{3+} compound. These results suggest that the Gd system is in a less polarizable environment indicating a lower covalent character of the metal–donor atom interaction.

All tungstate systems where the $\Omega_2 > \Omega_4$ parameters (Table 2) suggest that the coordination geometry is such that the higher rank components of these interactions have less values than the lower rank ones. Therefore, this might suggest that the site symmetry occupied by the Eu^{3+} ion in tungstate systems do not have a character of centrosymmetric chemical environment presenting the $\Omega_2 \gg 1 \times 10^{-20}$ cm^2 different from the $[Eu(H_2O)_6](ClO_4)_3$ complex in the O_h symmetry ($\Omega_2 = 1.1 \times 10^{-20}$ cm^2) [23]. It is important to consider that the $^5D_0 \rightarrow {}^7F_2$ transition is formally forbidden by electric dipole selection rule and the band related to this hypersensitive transition ($\Delta J = 2$) is absent when the europium ion lies on a center of inversion. The $RE_2(WO_4)_3$ compounds also shows a high value for the Ω_4 parameter suggesting a highly sensitive behavior of the $^5D_0 \rightarrow {}^7F_4$ transition ($\Delta J = 4$), possibly as a consequence of the basicity of the oxygen donor.

The highest values of the emission quantum efficiencies were obtained from the $RE_2(WO_4)_3$:Eu^{3+} (68% for La^{3+} and 64% for Gd^{3+}) are due to a significant decrease in non-radiative decay rates from the $^5D_0$ level as compared to the europium tungstate ($\eta = 19\%$). The CIE chromaticity coordinates at room temperature for $La_2(WO_4)_3$:Eu^{3+} are $x = 0.66$ and $y = 0.33$, while for $Gd_2(WO_4)_3$:Eu^{3+} they are $x = 0.66$ and $y = 0.34$. These chromaticity coordinates are excellent for a red phosphor and indicate that they are comparable to those of the commercially available red phosphor used for cathode ray tube (Y_2O_2S:Eu^{3+}; $x = 0.64$, $y = 0.34$) [5].

4. Conclusions

The $RE_2(WO_4)_3$:Eu^{3+} system (RE^{3+} = La and Gd) was prepared using the Pechini method. The infrared spectra indicate two types of WO_4 units. The presence of one peak assigned to the $^5D_0 \rightarrow {}^7F_0$ transition and a single-exponential fit from the luminescence decay curves of the emitting $^5D_0$ level, indicates the existence of only one symmetry site around the Eu^{3+} ion in these two systems. The emission spectra under excitation at the $O \rightarrow Eu^{3+}$ LMCT states (310 nm) show only transitions from the emitting $^5D_0$ level, whereas under excitation at $^7F_0 \rightarrow {}^5L_6$ transition of the Eu^{3+} ion (393 nm) show transitions arising from emitting $^5D_{0-3}$ levels. This phenomenon occurs due to a resonance crossover between the LMCT states and the emitting ^5D_J levels. The high values of the Ω_2 parameters for these systems suggest a high hypersensitive behavior of the $^5D_0 \rightarrow {}^7F_2$ transition. However, the Eu^{3+} ion in the $Eu_2(WO_4)_3$ compound is in a more polarizable environment than in $RE_2(WO_4)_3$:Eu^{3+} system, indicating a considerable covalent character of the metal–donor atom interaction in the europium tungstate compound.

The $RE_2(WO_4)_3$:Eu^{3+} systems have higher values of emission quantum efficiencies than the $Eu_2(WO_4)_3$ compound, suggesting that the doped systems are promising phosphors.

Acknowledgments

The authors are grateful to the Fundação de Amparo à Pesquisa do Estado de São Paulo (FAPESP) and the Conselho Nacional de Desenvolvimento Científico e Tecnológico (CNPq-RENAMI).

References

[1] C.R. Ronda, T. Jüstel, H. Nikol, J. Alloys Compounds 275–277 (1998) 669–676.
[2] K. Nassau, H. Levinstein, G.M. Loiacono, J. Phys. Chem. Solids 26 (1965) 1805.
[3] H.J. Borchardt, J. Chem. Phys. 39 (3) (1963) 504–511.
[4] D.H. Templeton, A. Zalkin, Acta Cryst. 16 (1963) 762–766.
[5] Y.R. Do, Y.D. Huh, J. Electrochem. Soc. 147 (11) (2000) 4385–4388.
[6] Y.H. Tseng, B.S. Chiou, C.C. Peng, L. Ozawa, Thin Solid Films 330 (1998) 173–177.
[7] U. Rambabu, P.K. Khanna, I.C. Rao, S. Buddhudu, Mater. Lett. 34 (1998) 269–274.
[8] L. Macalik, J. Hanuza, B. Macalik, W. Strek, J. Legendziewicz, Eur. J. Solid State Inorg. Chem. 33 (1996) 397–410.
[9] C.A. Kodaira, H.F. Brito, O.L. Malta, O.A. Serra, J. Lumin. 101 (1-2) (2003) 11–21.
[10] M.U. Pechini, US Patent No. 3330697, 1967.
[11] W. Liu, G.C. Farrington, F. Chaput, B. Dunn, J. Electrochem. Soc. 143 (3) (1996) 879–884.
[12] C. Laberty-Robert, F. Ansart, C. Deloget, M. Gaudon, A. Rousset, Mater. Res. Bull. 36 (2001) 2083–2101.
[13] P. Pramanik, Bull. Mater. Sci. 22 (3) (1999) 335–339.
[14] L.J. Burcham, I.E. Wachs, Spectrochim. Acta Part A 54 (1998) 1355–1368.
[15] J.P.M. van Vliet, D. van der Voort, G. Blasse, J. Lumin. 42 (1989) 305.
[16] W.H. Fonger, C.W. Struck, J. Chem. Phys. 52 (12) (1970) 6364–6372.
[17] G.F. de Sá, O.L. Malta, C.M. Donegá, A.M. Simas, R.L. Longo, P.A. Santa-Cruz, E.F. Silva Jr., Coord. Chem. Rev. 196 (2000) 165–195.
[18] O.L. Malta, H.F. Brito, J.F.S. Menezes, F.R.G. Silva, S. Alves Jr., F.S. Farias Jr., A.V.M. de Andrade, J. Lumin. 75 (1997) 255–268.
[19] H.F. Brito, O.L. Malta, J.F.S. Menezes, J. Alloys Compounds 303 (2000) 316–319.
[20] O.L. Malta, H.F. Brito, J.F.S. Menezes, F.R.G. Silva, C.M. Donegá, S. Alves Jr., Chem. Phys. Lett. 282 (1998) 233–238.
[21] O.L. Malta, W.M. de Azevedo, E.G. de Araújo, G.F. de Sá, J. Lumin. 26 (1982) 337–343.
[22] W.T. Carnall, H. Crosswhite, H.M. Crosswhite, Energy structure and transition probabilities of the trivalent lanthanides in LaF_3, Report, Argonne National Laboratory, 1977.
[23] E.E.S. Teotonio, J.G.P. Espínola, H.F. Brito, O.L. Malta, S.F. Oliveira, D.L.A. de Faria, C.M.S. Izumi, Polyhedron 21 (18) (2002) 1837–1844.